Brief communication

MOLECULAR METABOLISM

The diabetes medication Canagliflozin reduces cancer cell proliferation by inhibiting mitochondrial complex-I supported respiration

Linda A. Villani [1], Brennan K. Smith [1], Katarina Marcinko [1], Rebecca J. Ford [1], Lindsay A. Broadfield [1], Alex E. Green [1], Vanessa P. Houde [2], Paola Muti [2], Theodoros Tsakiridis [2], Gregory R. Steinberg [1,3,*]

ABSTRACT

Objective: The sodium-glucose transporter 2 (SGLT2) inhibitors Canagliflozin and Dapagliflozin are recently approved medications for type 2 diabetes. Recent studies indicate that SGLT2 inhibitors may inhibit the growth of some cancer cells but the mechanism(s) remain unclear.

Methods: Cellular proliferation and clonogenic survival were used to assess the sensitivity of prostate and lung cancer cell growth to the SGLT2 inhibitors. Oxygen consumption, extracellular acidification rate, cellular ATP, glucose uptake, lipogenesis, and phosphorylation of AMP-activated protein kinase (AMPK), acetyl-CoA carboxylase, and the p70S6 kinase were assessed. Overexpression of a protein that maintains complex-I supported mitochondrial respiration (NDI1) was used to establish the importance of this pathway for mediating the anti-proliferative effects of Canagliflozin.

Results: Clinically achievable concentrations of Canagliflozin, but not Dapagliflozin, inhibit cellular proliferation and clonogenic survival of prostate and lung cancer cells alone and in combination with ionizing radiation and the chemotherapy Docetaxel. Canagliflozin reduced glucose uptake, mitochondrial complex-I supported respiration, ATP, and lipogenesis while increasing the activating phosphorylation of AMPK. The overexpression of NDI1 blocked the anti-proliferative effects of Canagliflozin indicating reductions in mitochondrial respiration are critical for anti-proliferative actions.

Conclusion: These data indicate that like the biguanide metformin, Canagliflozin not only lowers blood glucose but also inhibits complex-I supported respiration and cellular proliferation in prostate and lung cancer cells. These observations support the initiation of studies evaluating the clinical efficacy of Canagliflozin on limiting tumorigenesis in pre-clinical animal models as well epidemiological studies on cancer incidence relative to other glucose lowering therapies in clinical populations.

Keywords AMP-activated protein kinase AMPK; Lipogenesis; SGLT2; Prostate cancer; Lung cancer; Breast cancer; Colon cancer; mTOR; Cancer metabolism; Glucose uptake

1. INTRODUCTION

Phlorizin is a non-selective inhibitor of the sodium-glucose transporters (SGLTs) that was first isolated from the bark of apple trees. While effective in lowering blood glucose by promoting glycosuria through the inhibition of SGLT2 in the kidney, it also causes gastrointestinal distress as it concurrently targets intestinal SGLT1 [1]. This adverse effect prompted the development of inhibitors with greater affinity for the SGLT2 isoform, such as Canagliflozin and Dapagliflozin, which have recently received approval in many countries for the treatment of type 2 diabetes as a monotherapy or in combination with the biguanide metformin [2].

In addition to treating diabetes, metformin also inhibits cancer cell growth [3] and is currently the subject of over 150 oncology trials [4]. While many molecular targets of metformin have been described, both its anti-diabetic and anti-cancer effects have been proposed to involve the inhibition of mitochondrial complex-I [5–7] and the subsequent activation of the 5′-adenosine monophosphate-activated protein kinase (AMPK) [5,8,9]. Similar results have been observed with PPAR gamma agonists [7,10,11]. AMPK is a master metabolic stress sensor in eukaryotic cells that inhibits energy-consuming processes and

[1]Department of Medicine, McMaster University, Hamilton, Ontario, L8K 4P1, Canada [2]Department of Oncology, McMaster University, Hamilton, Ontario, L8K 4P1, Canada [3]Department of Biochemistry and Biomedical Sciences, McMaster University, Hamilton, Ontario, L8K 4P1, Canada

*Corresponding author. Division of Endocrinology and Metabolism, Department of Medicine, McMaster University, 1280 Main St. West, Hamilton, Ontario, L8K 4P1, Canada. E-mail: gsteinberg@mcmaster.ca (G.R. Steinberg).

Abbreviations: 2-DG, 2-deoxy-D-glucose; ACC, acetyl-CoA carboxylase; AD-AMPKDN, adenoviral alpha-1 dominant negative; AD-CRE, adenoviral control; ACCDKI, ACC double knock-in (Ser79/212 Ala); AMPK, 5′-adenosine monophosphate-activated protein kinase; β1KO, AMPK β1-subunit knockout; ECAR, extracellular acidification rate; FBS, fetal bovine serum; mTORC1, mammalian target of rapamycin complex 1; OCR, oxygen consumption rate; PBS, phosphate buffered saline; SGLT1, sodium-glucose transporter 1; SGLT2, sodium-glucose transporter 2

Received July 22, 2016 • Revision received August 14, 2016 • Accepted August 18, 2016 • Available online 26 August 2016

http://dx.doi.org/10.1016/j.molmet.2016.08.014

increases catabolic processes to restore cellular energy homeostasis [12,13]. This is achieved, in part, by inhibiting anabolic pathways including the synthesis of proteins and lipids by limiting the activity of the mammalian target of rapamycin complex 1 (mTORC1) and acetyl-CoA carboxylase (ACC), respectively [14–16]. Notably, these two pathways are commonly upregulated in many cancers [17,18]. Given these attributes, the inhibition of mitochondrial function and activation of AMPK may be important for limiting the growth of a variety of cancer types, a concept which is consistent with recent studies indicating that preservation of mitochondrial respiration blocks the inhibitory effects of biguanides on cellular proliferation [19,20].

Recent studies indicated that the SGLT2 inhibitors Canagliflozin and Dapagliflozin may inhibit the growth of pancreatic and colon cancer cells, potentially through inhibition of SGLT2-mediated glucose uptake [22,23]. However, in many tumors, the inhibition of glucose uptake alone is not sufficient to reduce cell viability/proliferation [24,25]; thus, it is unclear whether this is the primary mechanism by which SGLT2 inhibitors limit growth. We have recently observed that Canagliflozin activates AMPK by inhibiting mitochondrial respiration in human embryonic kidney cells and primary mouse hepatocytes [26]. In the current study, we find that clinical concentrations of Canagliflozin, but not Dapagliflozin, potently inhibit the growth of cancer cells and potentiate the effects of cytotoxic therapies. These anti-cancer properties are dependent on the inhibition of complex-I supported mitochondrial respiration but not the activation of AMPK. These data indicate that, like biguanides, Canagliflozin inhibits mitochondrial respiration and cellular proliferation, suggesting that this type 2 diabetes medication may also have utility in preventing and treating cancer.

2. MATERIALS AND METHODS

2.1. Cell lines, culture conditions and treatments

Human prostate (PC3, 22RV-1), lung (A549, H1299), breast (MCF-7), colon (HCT116), liver (HepG2) and ovarian (SKOV-3) cancer cells were purchased from the American Type Culture Collection (ATCC: Manassa, VA). Phoenix-AMPHO cells were a kind gift from Dr. Xu-Dong Zhu. Immortalized mouse embryonic fibroblast (MEF) cells were produced from primary MEF cells acquired from WT, AMPK β1KO, and ACC double knock-in (DKI, genetic disruption of AMPK inhibitory phosphorylation sites on ACC1/2 (Ser79/212Ala)) mice as described [15]. A549, H1299, PC3, 22RV-1, HCT116 and SKOV-3 cells were cultured in RPMI 1640 media, HepG2 and MCF-7 cells were cultured in MEM media, and Phoenix-AMPHO and MEF cells were cultured in DMEM media (Gibco: Mississauga, ON). Culture media were supplemented with 10% (v/v) FBS and 1% (v/v) antibiotic-antimycotic (100×) (Gibco: Mississauga, ON). MCF-7 media was also supplemented with 1% (v/v) non-essential amino acids (100×) and 1% (v/v) sodium-pyruvate (100×) (Gibco: Mississauga, ON). All cells were maintained at 37 °C in 5% CO_2. The NDI1 and control (pMXS) vectors were created as previously described [20] and amplified in Phoenix-AMPHO cells. Parental PC3 cells were infected to generate PC3-NDI1 and PC3-pMXS stably transfected cell lines and maintained in 0.75 mM glucose as described [20] before treatment with Canagliflozin and Phenformin for 4 h (lipogenesis assay) or 48 h (proliferation assay). The AMPK α1 dominant negative was created as previously described [27]. PC3 cells were infected with adenovirus containing AdCre (control, AD-CRE) or AMPK-α1 threonine 172 to aspartic acid (T172D) dominant negative (AD-AMPKDN) as previously described [28] and treatments started 24 h post-infection. Media was supplemented with Galactose, Na-Pyruvate or Na-Acetate (Sigma: Toronto, ON) as indicated. Cells were treated as described with Canagliflozin or Dapagliflozin (Selleck Chemicals LLC), Docetaxel (Cayman: Ann Arbor, MI), ionizing radiation or controls (Salicylate, Phenformin, Sigma: Toronto, ON). Working solutions were prepared so that the vehicle comprised less than 0.1% of the media.

2.2. Clonogenic survival assay

Cells were seeded at a density of 500–1000 cells/well into 12-well plates and treated in triplicate. Colonies were allowed to form over 5–10 days. Cells were fixed and stained with 0.5% crystal violet DNA stain (Sigma: Toronto, ON) in 50% EtOH. Viable colonies (≥50 cells) were counted.

2.3. Proliferation assay

Cells were seeded at a density of 1000–2000 cells/well into 96-well plates and treated in quadruplicate for 48–72 h. Cells were fixed with 10% formalin and stained with 0.5% crystal violet DNA stain in 20% MeOH. Once dry, the intracellular stain was solubilized with 0.05 M NaH_2PO_4 and the absorbance at 570 nm was measured.

2.4. Cell viability assay

Cells were seeded at a density of 6×10^4 cells/well into 6-well plates and treated in duplicated. Cell viability of floating and adherent cells was determined by trypan blue (Gibco: Mississauga, ON) exclusion according to the manufacturer's protocol after 72 h.

2.5. Lipogenesis assay

Cells were treated in triplicate with drugs prepared in 0.5 mM Na-acetate and 10 μCi/mL [H^3]-Na-acetate (Perkin Elmer) in supplemented media. After 4 h, plates were placed on ice, washed with ice cold PBS, and snap frozen to physically disrupt cell membranes. Cells were collected at room temperature and a methanol: chloroform (2:1) solvent was used for lipid extraction as previously described [29].

2.6. 2-Deoxy-D-glucose uptake

Cells were treated in triplicate with drugs prepared in 2 nCi [H^3]-2-DG (Perkins Elmer) in HEPES buffer (140 mM NaCl, 20 mM HEPES-Na, 5 mM KCl, 2.5 mM $MgSO_4$, 1 mM $CaCl_2$, pH 7.4). After 10 min, plates were placed on ice, washed with ice cold PBS, and snap frozen in lysis buffer. Lysates were collected on ice and measured for radioactive counts.

2.7. Extracellular acidification assay

Cells were seeded at a density of 2.25×10^5 cells/well into 48-well plates in quadruplicate. Once adherent, cells were washed with PBS and incubated with "test media": (bicarbonate-free, pyruvate-free DMEM supplemented with 11 mM Glucose, 2 mM L-Glutamine and 25 mg/L phenol red, pH 7.8) in a SpectraMax M5/M5e microplate reader at 37 °C. The ΔOD 560–480 nm was measured in 9 locations per well, every 5 min over 4 h. Treatments were injected into wells 1 h into the incubation period. ECAR was determined by measuring rate of change of the test media color.

2.8. Respiration assay

High-resolution respirometry was conducted on approximately 2.5×10^6 cells in duplicate, at 37 °C (Oroboros Oxygraph-2k: Innsbruck, Austria). Cells were washed with PBS, collected in MiR05 buffer (110 mM sucrose, 60 mM potassium lactobionate, 20 mM HEPES, 10 mM KH_2PO_4, 3 mM $MgCl_2$, 0.5 mM EGTA, 1 g/L BSA, pH 7.1), and added to the chambers. Cells were permeabilized with Digitonin (10 μg/million cells, Sigma: Toronto, ON) and then treated with

glutamate (5 mM), malate (2 mM) and ADP (5 mM) to measure complex-I supported respiration (GMD), which was subsequently confirmed through blockade with the complex-I specific inhibitor rotenone (0.5 μM). The change in respiration between GMD and the residual respiration after treatment with rotenone was used for analysis. Cells were treated with succinate (10 mM) to measure complex-II supported respiration, which was later inhibited by the complex-II specific inhibitor malonate (5 mM). The change in respiration between succinate stimulated respiration, and the residual respiration after malonate treatment was used for analysis.

2.9. Cellular ATP assay

Cells were seeded at a density of 2×10^4 cells/well into white-walled 96-well plates and treated in duplicate for 30 min. The Abcam Luminescent ATP Detection Kit (ab113849) was used according to the manufacturer's protocol.

2.10. Quantitative real-time PCR

A Roche High Pure RNA Isolation Kit was used to extract RNA from cells. To eliminate genomic DNA, samples were incubated with a solution of DNase I endonuclease. RNA quantity (ng/μL) and purity (A260/A280) were assessed using a spectrophotometer. cDNA was synthesized using SuperScript III reverse transcriptase (Life Technologies #18080-044) according to the manufacturer's protocol. Amplification and detection was performed using a qPCR thermocycler (Corbett Rotor Gene 6000), TaqMan probes (*SLC5A2* # Hs00894642_m1, *18S* # Hs99999901_s1) and TaqMan MasterMix (#4369016). Values were corrected to a housekeeping gene (18S). The expression of the gene of interest was calculated using the $2^{-\Delta\Delta Ct}$ approach.

2.11. Western blotting and densitometry

Cells were treated in duplicate, washed in ice-cold PBS, and collected in ice-cold lysis buffer (1 mM DTT, 1 mM Na_3VO_4, 20% triton-X, 1% protease inhibitor cocktail tablet (Roche), 50 mM HEPES, 150 mM NaCl, 100 mM NaF, 10 mM Na pyrophosphate, 5 mM EDTA, 250 mM Sucrose). Samples were snap frozen, thawed, and manually collected on ice. Working samples were prepared with 4× SDS sample buffer (8% SDS, 0.25% Bromophenol Blue, 35% Glycerol, 250 mM Tris—HCl (pH 6.8), 1:20 1 M DTT). Boiled protein sample was separated using SDS-PAGE. Proteins were electrically transferred at 4 °C onto a nitrocellulose membranes using 10% (v/v) MeOH transfer buffer. Membranes were blocked (5% BSA solution in TBST (50 mM Tris, 150 mM NaCl, 1 M HCl, pH 7.4, 0.1% Tween-20)) and incubated with the indicated primary and complementary HRP-conjugated secondary antibodies. Antibodies were purchased from Cell Signaling Technology. Densitometry values were quantified using Image J software (McMaster University Biophotonics Lab, Hamilton, ON) and are expressed as percent of control.

2.12. Xenograft model and tissue handling

The McMaster University Animal Ethics Research Board approved all animal procedures. Male BALB/c-Nude mice (5 week, Charles-River: Mississauga, ON) were housed in a pathogen-free facility under a 12 h light/dark cycle at 23 °C, with *ad libitum* access to radiated chow and water. Mice were subcutaneously grafted with 1×10^6 PC3 cells into the right and left flank. Tumor dimensions were measured with a caliper. Volumes were calculated using the following equation: $1/2(W^2 \times L)$, where W and L are the measured width and length, respectively. When tumor volumes reached 100—150 mm^3, mice were randomly divided into two groups: (1) vehicle (saline solution containing 0.5% carboxymethyl cellulose, 0.025% Tween-20) or (2) 100 mg/kg Canagliflozin. Mice were fasted overnight (12 h) and re-fed with chow for 2 h before being gavaged with either Canagliflozin or vehicle (10 μL/g body weight). Food was withdrawn again during the 5-hour treatment. Tumors were then extracted and immediately snap frozen in liquid nitrogen. Tumors were crushed, collected in lysis buffer and immediately homogenized for protein extraction and western blotting analysis.

2.13. Statistical analysis

All results are expressed as a mean with standard error of the mean (SEM). A p value <0.05 was considered significant (*). Statistical analyses were performed using student t-test, one-way or two-way ANOVA as appropriate. Bonferroni's or Fisher LSD multiple comparison tests were used after the ANOVA. Clonogenic and proliferative IC50 values were calculated using a non-linear regression model with normalized slope.

3. RESULTS

3.1. Canagliflozin blocks the cellular proliferation and clonogenic survival of cancer cells

Clinically achievable concentrations of Canagliflozin and Dapagliflozin range from 5 to 30 μM [2]. We found that within this clinical window of exposure, Canagliflozin, but not Dapagliflozin, inhibited the proliferation and clonogenic survival of prostate (Figure 1A—B) and lung (Figure 1C—D) cancer cells. These inhibitory effects were not due to reductions in cell viability (Figure 1E). Similar observations were made in cells derived from liver (HepG2) and breast (MCF7) cancers, while the growth of those derived from colon (HCT116) and ovarian (SKOV-3) cancers could only be inhibited at higher doses (Figure S1A—D). Docetaxel and ionizing radiation induce cell death through microtubule stabilization and the production of double stranded DNA breaks, respectively, and are standard therapies for many cancers. We show that the addition of Canagliflozin improved the efficacy of both of these treatments in prostate cancer cells (Figure 1F—G). These data indicate that clinically relevant concentrations of Canagliflozin, but not Dapagliflozin, potently suppress proliferation and clonogenic survival of cancer cells alone and in combination with cytotoxic therapies.

3.2. Canagliflozin rapidly activates AMPK in cancer cells *in vitro* and *in vivo*

While others [22] have reported the expression of SGLT2 in some cancer cells, we observed very low mRNA expression in prostate and lung cancer cells (Figure S2A), a finding consistent with the protein atlas database [30]. However, despite low levels of SGLT2 expression we found that Canagliflozin, but not Dapagliflozin, acutely and dose-dependently decreased 2-deoxy-D-glucose (2-DG) uptake (Figure S2B). To examine whether this inhibition of glucose uptake may be important for the anti-proliferative effects of Canagliflozin, we compared the proliferation of cells grown in standard media (11 mM) to those grown in low glucose media (0.75 mM) or standard media supplemented with pyruvate or acetate. We hypothesized that if Canagliflozin inhibited cell growth through inhibition of glucose uptake then these effects would be amplified under low glucose conditions and diminished following supplementation with pyruvate or acetate. Instead, we found that the anti-proliferative effects of Canagliflozin were similar under low glucose and pyruvate or acetate supplemented conditions over 72 h, suggesting that the acute attenuation of glucose uptake is not the primary factor suppressing proliferation (Figure S2C—D).

The inhibition of complex-I supported respiration can limit cellular proliferation [19—21]. To examine whether this might be important for

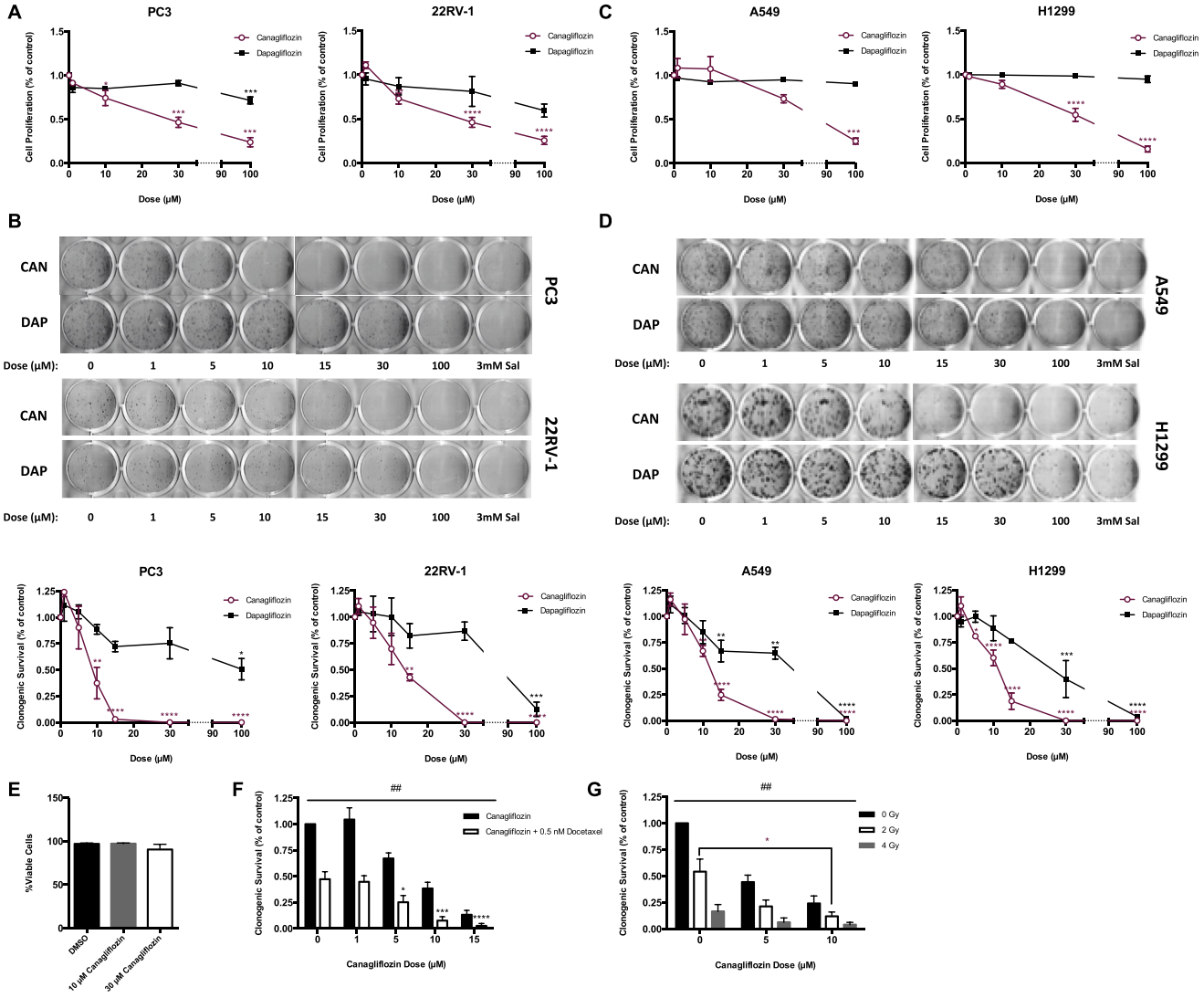

Figure 1: Clinically effective concentrations of Canagliflozin inhibit the proliferation and clonogenic survival of cancer cells. (A) Cellular proliferation of prostate cancer cells (PC3 and 22RV-1) treated with Canagliflozin and Dapagliflozin and expressed relative to the vehicle controls for 72 h (n = 3, in quadruplicate). (B) Clonogenic survival of prostate cancer cells treated with Canagliflozin, Dapagliflozin or Salicylate and expressed relative to the vehicle controls. Representative images above and quantifications (n = 3, in triplicate) shown below. (C) Cellular proliferation of lung cancer cells (A549 and H1299) treated with Canagliflozin and Dapagliflozin and expressed relative to the vehicle controls for 72 h (n = 3, in quadruplicate). (D) Clonogenic survival of lung cancer cells treated with Canagliflozin, Dapagliflozin, or Salicylate and expressed relative to the vehicle controls. Representative images above and quantifications (n = 3, in triplicate) shown below. (E) Percentage of viable PC3 cells treated with Canagliflozin or vehicle over 72 h (n = 5, in duplicate). (F) Clonogenic survival of PC3 cells treated with Canagliflozin as a single agent or in combination with 0.5 nM Docetaxel (n = 3, in triplicate). (G) Clonogenic survival of PC3 cells treated with Canagliflozin as a single agent or in combination with 0, 2 or 4 Gy of radiation (n = 3, in triplicate). Results are expressed as the mean and standard error of the mean (SEM). Vehicle versus treatment * = $p < 0.05$, ** = $p < 0.01$, *** = $p < 0.001$, **** = $p < 0.0001$ by one-way ANOVA for A–D, by two-way ANOVA for F–G. Single versus combination treatment ## = $p < 0.01$ by two-way ANOVA for F–G.

mediating the effects of Canagliflozin, prostate cancer cells were grown in galactose, a method used to enhance cellular reliance on oxidative phosphorylation for ATP production [31]. When cells were grown with galactose, Canagliflozin was approximately 50% more efficient at inhibiting growth compared to glucose alone (Figure 2A). Similar effects were observed in H1299 lung cancer cells (Figure S2E). Canagliflozin reduced cellular ATP under normal glucose conditions, and this effect was more dramatic when cells were cultured in growth media containing galactose (Figure 2B). Similar observations were made with the biguanide phenformin (Figure 2B), suggesting that Canagliflozin may be inhibiting mitochondrial respiration.

AMPK is acutely activated by reductions in cellular ATP [32]. We found that Canagliflozin increased the activating phosphorylation of AMPK (Thr172) by ~4-fold within 30 min of treatment, an effect which was maintained up to 24 h (Figure 2C–G). Canagliflozin also increased the phosphorylation of ACC (Ser79) by ~8-fold over the treatment period. AMPK inhibits the activity of mTOR, and, consistent with this effect, Canagliflozin rapidly decreased the phosphorylation of S6K (Thr389) and its substrate S6 (Ser 240/244) by approximately 50%. In contrast, Dapagliflozin did not alter the phosphorylation status of AMPK, ACC, S6K, or S6 (Figure S3A–E). Given the rapid activation of AMPK, we subsequently performed a dose–response with both SGLT2 inhibitors at 0.5 h and found that, consistent with the inhibition of proliferation and clonogenic survival, Canagliflozin, but not Dapagliflozin, dose-dependently increased the phosphorylation of AMPK and ACC (Figure 2H–J and Figure S3F–H). Consistent with increased ACC

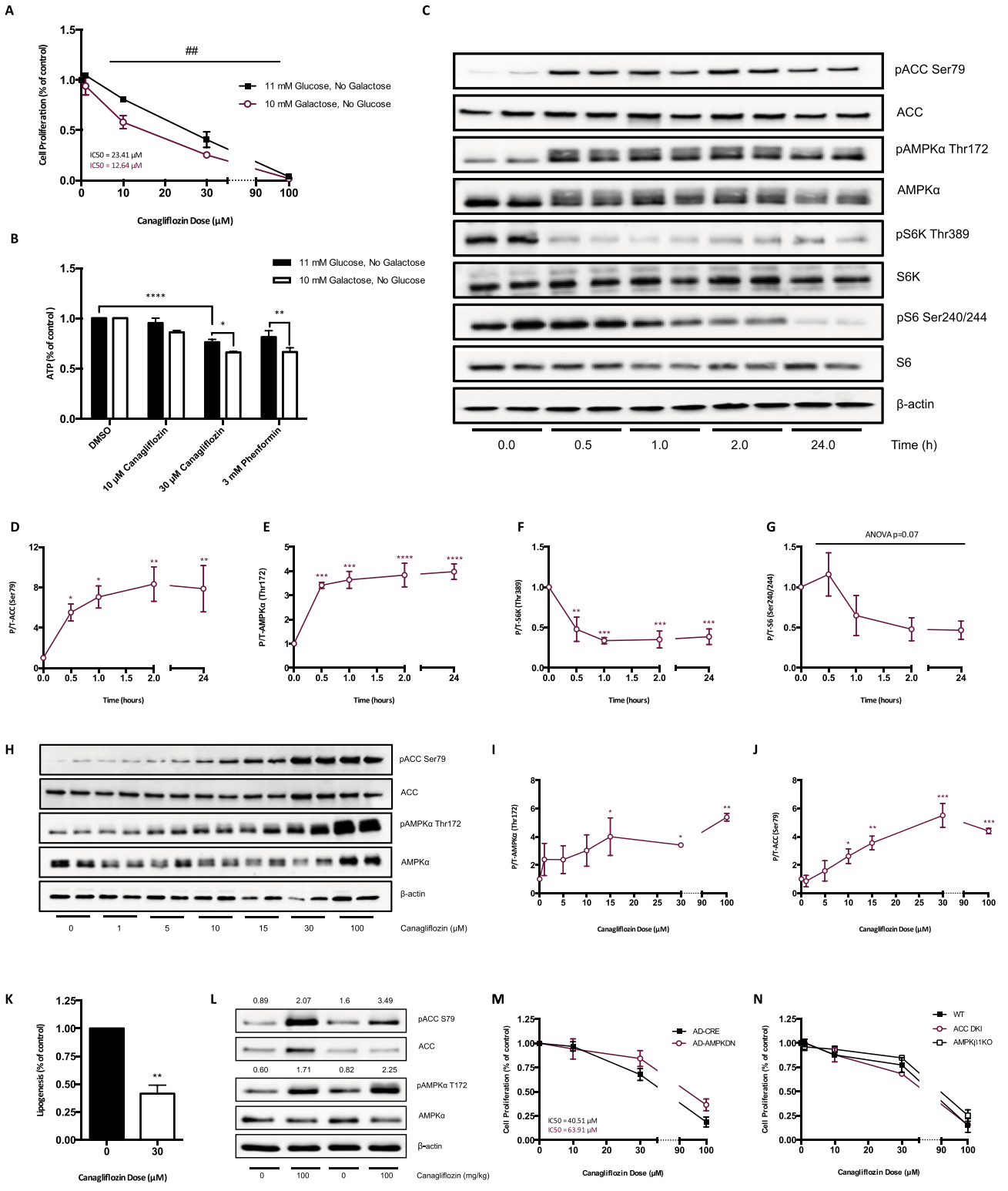

Figure 2: Canagliflozin activates AMPK in cancer cells *in vitro* and *in vivo*. (A) Cellular proliferation of PC3 cells maintained in 11 mM glucose or 10 mM galactose, treated with Canagliflozin and expressed relative to the vehicle controls for 72 h (n = 3, in quadruplicate). (B) Cellular ATP (μM) in PC3 cells maintained in 11 mM glucose or 10 mM galactose for 24 h, then treated with Canagliflozin or Phenformin for 30 min and expressed relative to the vehicle controls (n = 4, in duplicate). (C) Representative western blot of Canagliflozin treated PC3 cells. Canagliflozin (30 μM) increases pAMPK and pACC and reduces pS6k and pS6. (D–G) Quantification of (C) (n = 3–6, in duplicate). (H) Canagliflozin dose-dependently increases pAMPK and pACC in PC3 cells after 30 min (I–J). Quantification of (H) (n = 3–6, in duplicate). (K) Rate of lipogenesis (nmol of H^3-acetate incorporation into fatty acid/mg of protein/hour) in PC3 cells treated with Canagliflozin (30 μM) for 4 h relative to the vehicle control (n = 3, in triplicate). (L) 100 mg/kg Canagliflozin administered by oral gavage increases pAMPK and pACC in PC3 xenografts of BALB/c-nude mice (densitometry units of pACC/ACC and pAMPK/AMPK stated above blot image). (M) Cellular proliferation of PC3 cells infected with empty vector (AD-CRE) or dominant negative AMPK (AD-AMPKDN), treated with Canagliflozin and expressed relative to vehicle controls for 72 h (n = 6, in quadruplicate). (N) Cellular proliferation of WT, ACCDKI and AMPK β1KO MEF cells treated with Canagliflozin and expressed relative to the vehicle controls for 72 h (n = 3, in quadruplicate). Results are expressed as the mean and standard error of the mean (SEM). Galactose versus glucose ## = $p < 0.01$ by two-way ANOVA for A, * = $p < 0.05$, ** = $p < 0.01$, **** = $p < 0.0001$ by two-way ANOVA for B. Vehicle versus treatment * = $p < 0.05$, ** = $p < 0.01$, *** = $p < 0.001$, **** = $p < 0.0001$ by one-way ANOVA for D–G and I–J, by t-test for K.

phosphorylation and reductions in cellular ATP, Canagliflozin potently inhibited the synthesis of fatty acids derived from acetate (Figure 2K), indicating that the inhibition of lipogenesis was not related to the reductions in glucose uptake. Importantly, this activation of AMPK was also observed in PC3 xenografts following a single oral dose of Canagliflozin (Figure 2L). However, this activation of AMPK did not appear to be essential for mediating the anti-proliferative effects of Canagliflozin, as they were not significantly altered when a dominant-negative AMPK was overexpressed (Figure 2M). Furthermore, the anti-proliferative effects of Canagliflozin were comparable between mouse embryonic fibroblasts derived from wildtype mice or those lacking the β1 subunit of AMPK (AMPK β1KO [15,33]) or the key regulatory AMPK phosphorylation sites on ACC (ACCDKI [29]), which are essential for AMPK regulation of lipid synthesis (Figure 2N).

3.3. Inhibition of complex-I supported respiration is important for the anti-proliferative effects of Canagliflozin

Recent studies have indicated that the inhibition of mitochondrial complex-I is vital for mediating the anti-proliferative effects of biguanides [19,20] and that these effects are independent of AMPK [21]. We examined the effects of Canagliflozin on oxidative phosphorylation in cancer cells grown under standard glucose conditions and found that it induced greater acidification of the media compared to vehicle or Dapagliflozin (Figure 3A). We then examined respiration using permeabilized PC3 prostate cancer cells (a method which is not dependent on substrate delivery) and found that Canagliflozin dose-dependently reduced oxygen consumption through inhibition of complex-I (starting at concentrations as low as 5 μM) without affecting complex-II (Figure 3B–C). In contrast, Dapagliflozin had minimal effects on complex-I supported respiration within the therapeutic window of exposure and did not affect complex-II (Figure 3B–C).

To establish whether the inhibition of complex-I was important for mediating the anti-lipogenic and anti-proliferative effects of Canagliflozin, we expressed the *Saccharomyces cerevisiae* NADH dehydrogenase NDI1 (Figure 3D), which can maintain respiration in the presence of complex-I inhibitors (including rotenone, or biguanides) in mammalian cells [19,20,34]. Remarkably, we found that expression of NDI1 rescued the inhibitory effects of Canagliflozin on lipogenesis (Figure 3E) and made cells completely refractory to the inhibitory effects of Canagliflozin on cellular proliferation compared to controls (Figure 3F). These data indicate that Canagliflozin limits cancer cell proliferation by inhibiting complex-I supported respiration.

4. DISCUSSION

We find that Canagliflozin, but not Dapagliflozin, inhibits the proliferation and clonogenic survival of prostate and lung cancer cells. Canagliflozin also enhanced the effectiveness of Docetaxel and ionizing radiation to inhibit clonogenic survival. Despite similar potencies for inhibiting SGLT2 [2], Canagliflozin, but not Dapagliflozin, decreased 2-DG uptake, inhibited complex-I supported mitochondrial respiration, reduced cellular ATP, and activated AMPK. Activation of AMPK was also observed in cancer xenographs following an acute oral gavage of mice with Canagliflozin. Importantly, the anti-proliferative effects of Canagliflozin were completely reversed following overexpression of NDI1, thus indicating that the inhibition of mitochondrial complex-I is required for the inhibitory effects of Canagliflozin on cancer cell proliferation.

The anti-proliferative effects of Canagliflozin were similar under both high and low glucose conditions and following supplementation of the media with pyruvate or acetate, suggesting substrate for oxidative phosphorylation or lipogenesis was not the primary factor limiting proliferation. Previous studies have shown that compared to Dapagliflozin, Canagliflozin has a higher affinity for inhibiting SGLT1 [2], and may also inhibit the glucose transporter GLUT1 [35]. While both SGLT1 [36] and GLUT1 [37] may be expressed in prostate cancer cells, previous studies have indicated that inhibiting glucose uptake in PC3 cells is insufficient to inhibit cellular proliferation [24]. Collectively, these data suggest that the inhibition of glucose uptake is unlikely to be the primary mechanism mediating the inhibition of cellular proliferation; however, as discussed below, it may be an important contributing factor.

We found that Canagliflozin increased media acidification and reduced ATP levels under standard glucose conditions, effects that were associated with the inhibition of mitochondrial complex-I. The anti-proliferative effects of Canagliflozin were also enhanced when the media was switched to galactose, a fuel that yields no net ATP when oxidized through glycolysis, suggesting that the inhibition of mitochondrial respiration was responsible for mediating the anti-proliferative effects. Consistent with this concept when the block in complex-I was circumvented by the expression of NDI1, Canagliflozin failed to decrease cellular proliferation. These data indicate that the inhibition of complex-I is vital for Canagliflozin to inhibit cellular proliferative capacity, but it is possible that simultaneous reductions in glucose uptake may also be important. For example, inhibiting glucose uptake with 2-DG and blocking complex-I supported respiration simultaneously with either metformin or rotenone dramatically enhances the ability of complex-I inhibitors to reduce cellular proliferation [25]. These data suggest that since Canagliflozin inhibits both glucose uptake and complex-I supported respiration simultaneously, this dual mechanism of action may be important for mediating the inhibitory effects on proliferation. The structural components that differentiate Canagliflozin from Dapagliflozin to mediate these effects of on glucose uptake and mitochondrial respiration are currently unknown but will be the subject of future studies.

Consistent with the effects of clinically relevant concentrations of Canagliflozin on inhibiting mitochondrial function and reducing cellular ATP, we find that it rapidly and robustly increased AMPK activity in cultured cells *in vitro*. Importantly, this effect was also observed in cancer xenographs following a single, acute oral gavage to mice. The activation of AMPK by Canagliflozin also increased phosphorylation of ACC at Ser79, a site that is regulated by AMPK to inhibit lipid synthesis [29]. However, in contrast to the effects observed when overexpressing NDI1, overexpressing a dominant negative AMPK or blocking AMPK's ability to phosphorylate and inhibit ACC did not impair Canagliflozin's ability to reduce cellular proliferation. Consistent with an AMPK-independent effect, Canagliflozin also inhibited the growth of A549 cells, which lack the upstream AMPK activator and tumor suppressor liver kinase B1 (LKB1) [13]. These data suggest that the activation of AMPK and phosphorylation of ACC are not essential for the anti-proliferative effects of Canagliflozin, findings that are consistent with a recent study indicating that blocking mitochondrial function, but not AMPK, is critical for mediating the anti-proliferative effects of metformin [21]. These findings are also consistent with the observed reduction in cellular ATP induced by Canagliflozin and previous observations that ATP is a vital cofactor for lipid synthesis that is required for cellular proliferation [38,39]. In addition, the inhibition of complex-I supported respiration also increases the production of reactive oxygen species and reduces cancer cell growth [40], suggesting this may be an additional mechanism by which Canagliflozin exerts anti-proliferative effects.

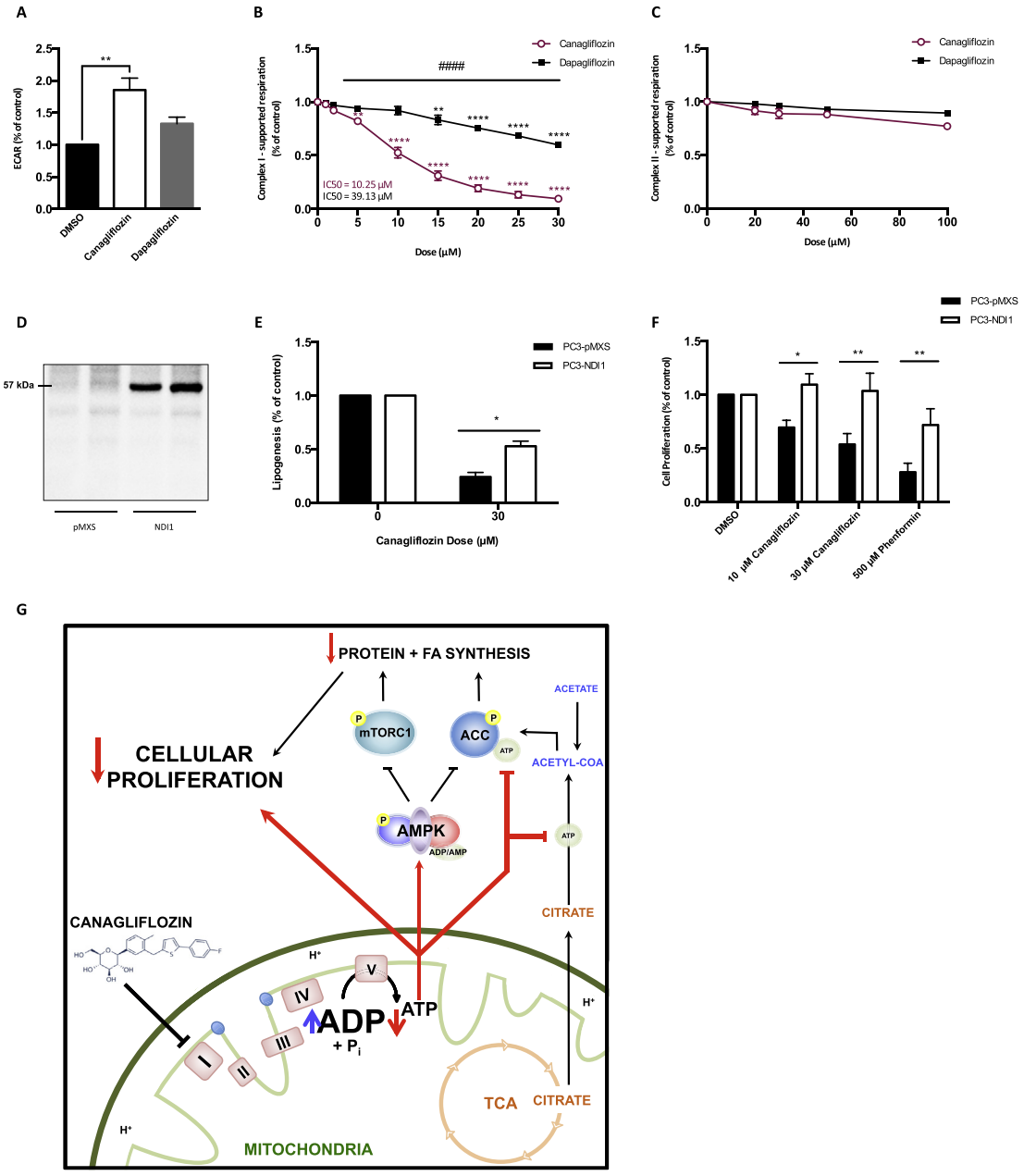

Figure 3: Canagliflozin inhibits mitochondrial complex-I to limit cancer cell proliferation. (A) Extracellular acidification rate (ECAR, mOD/min) of PC3 cells 3 h post treatment with Canagliflozin (30 µM), Dapagliflozin (30 µM), or vehicle (n = 4, in quadruplicate). (B) Rate of oxygen consumption (pmol/s/10^6 cells) through complex-I of permeabilized PC3 cells treated with increasing concentrations of Canagliflozin and Dapagliflozin (n = 4, in duplicate). (C) Rate of oxygen consumption (pmol/s/10^6 cells) through complex-II of permeabilized PC3 cells treated with increasing concentrations of Canagliflozin and Dapagliflozin (n = 4, in duplicate). (D) Western blot analysis of NDI1 expression in PC3-pMXS and PC3-NDI1 cells. (E) Rate of lipogenesis (nmol of [H^3-acetate] incorporation into fatty acid/mg of protein/hour) in PC3-pMXS and PC3-NDI1 cells treated with Canagliflozin (30 µM) for 4 h relative to the vehicle control (n = 3, in triplicate). (F) Cellular proliferation of PC3-PMXS and PC3-NDI1 cells treated with Canagliflozin or Phenformin and expressed relative to the vehicle controls for 48 h (n = 4, in quadruplicate). (G) Graphical representation of the proposed mechanism of Canagliflozin. Results are expressed as the mean and standard error of the mean (SEM). Vehicle versus treatment ** = $p < 0.01$, *** = $p < 0.001$, **** = $p < 0.0001$ by one-way ANOVA for A, by two-way ANOVA for B. Canagliflozin versus Dapagliflozin #### = $p < 0.0001$ by two-way ANOVA for B. pMXS versus NDI1 * = $p < 0.05$, ** = $p < 0.01$ by t-test for E, by two-way ANOVA for F.

5. CONCLUSION

Targeting mitochondrial energetics and metabolic checkpoints has emerged as an important modality for treating a multitude of cancers [15,41]. Our findings indicate that clinically achievable concentrations of Canagliflozin inhibit multiple pathways essential for cancer cell proliferation. Future studies examining the effects of Canagliflozin on cancer xenograph growth in SGLT2 null mice will be important to determine the impact of this therapy on cancer growth independently of systemic reductions in circulating blood glucose induced by glycosuria. Our studies also support the initiation of epidemiological studies examining the effects of Canagliflozin on cancer incidence relative to other glucose lowering therapies in patients with diabetes. These studies may lay the foundation for clinical trials investigating the

use of this well-tolerated therapy alone and in combination with other standard of care treatments.

AUTHORS' CONTRIBUTIONS

LAV, AEG, TT, PM, and GRS conceived and designed the study. LAV, BKS, KM, RJF, LAB, and VPH preformed experiments. LAV analyzed data. LAV, TT, PM, and GRS interpreted results of experiments. LAV and GRS prepared figures and drafted the manuscript. LAV, BKS, KM, RJF, LAB, VPH, AEG, PM, TT, and GRS edited and revised manuscript. All authors read and approved the final manuscript.

ACKNOWLEDGEMENTS

These studies were funded in part by a grant from the Canadian Cancer Society grant number P#20001191. We thank Miss Emily Day and Mrs. Vivian Leong for their technical assistance. We thank Dr. Sabatini (MIT) for providing the NDI1 and pMXS plasmids. B.K.S. is a recipient of a CIHR post-doctoral fellowship. A.E.G. is a recipient of a CIHR/MitoCanada Doctoral Research Award. G.R.S. is a Canada Research Chair in Metabolism and Obesity and the J. Bruce Duncan Chair in Metabolic Diseases.

APPENDIX A. SUPPLEMENTARY DATA

Supplementary data related to this article can be found at http://dx.doi.org/10.1016/j.molmet.2016.08.014.

CONFLICT OF INTEREST

The authors declare no conflict of interest.

REFERENCES

[1] White, J.R., 2010. Apple trees to sodium-glucose co-transporter inhibitors: a review of SGLT2 inhibition. Clinical Diabetes 28:5—10.
[2] Scheen, A.J., 2015. Pharmacodynamics, efficacy and safety of sodium-glucose co-transporter type 2 (SGLT2) inhibitors for the treatment of type 2 diabetes mellitus. Drugs 75:33—59.
[3] Pollak, M., 2013. Potential applications for biguanides in oncology. Journal of Clinical Investigation 123:3693—3700.
[4] ClinicalTrials.gov. Bethesda, 2016. https://clinicaltrials.gov [accessed 05.05.16].
[5] Foretz, M., Giugas, B., Bertrand, L., Pollak, M., Viollet, B., 2014. Metformin: from mechanisms of action to therapies. Cell Metabolism 20:953—966.
[6] Owen, M., Doran, E., Halestrap, E., 2000. Evidence that metformin exerts its anti-diabetic effects through inhibition of complex 1 of the mitochondrial respiratory chain. Biochemical Journal 348:607—614.
[7] Brunmair, B., Staniek, K., Gras, F., Scharf, N., Althaym, A., Clara, R., et al., 2004. Thiazolidinediones, like metformin, inhibit respiratory complex I. Diabetes 53:1052—1059.
[8] Zhou, G., Myers, R., Li, Y., Chen, Y., Shen, X., Frenyk-Melody, J., et al., 2001. Role of AMP-activated protein kinase in mechanism of metformin action. Journal of Clinical Investestigation 108:1167—1174.
[9] Zakikhani, M., Dowling, R., Fantus, I.G., Sonenberg, N., Pollak, M., 2006. Metformin is an AMP kinase-dependent growth inhibitor for breast cancer cells. Cancer Research 66:10269—10273.
[10] Fryer, L.G., Parbu-Patel, A., Carling, D., 2002. The anti-diabetic drugs rosiglitazone and metformin stimulate AMP-activated protein kinase through distinct signaling pathways. Journal of Biological Chemistry 28:25226—25232.
[11] Hawley, S.A., Gadalla, A.E., Olsen, G.S., Hardie, D.G., 2002. The antidiabetic drug metformin activates the AMP-activated protein kinase cascade via an adenine nucleotide-independent mechanism. Diabetes 8:2420—2425.
[12] Steinberg, G.R., Kemp, B.E., 2009. AMPK in health and disease. Physiological Reviews 89:1025—1078.
[13] Shackelford, D.B., Shaw, R.J., 2009. The LKB1—AMPK pathway: metabolism and growth control in tumour suppression. Nature Reviews Cancer 9:563—575.
[14] Shaw, R.J., 2009. LKB1 and AMP-activated protein kinase control of mTOR signalling and growth. Acta Physiologica (Oxford, England) 196:65—80.
[15] O'Brien, A.J., Villani, L.A., Broadfield, L.A., Houde, V.P., Galic, S., Blandino, G., et al., 2015. Salicylate activates AMPK and synergizes with metformin to reduce the survival of prostate and lung cancer cells ex vivo through inhibition of de novo lipogenesis. Biochemical Journal 469:177—187.
[16] Faubert, B., Boily, G., Izreig, S., Griss, T., Samborska, B., Dong, Z., et al., 2013. AMPK is a negative regulator of the warburg effect and suppresses tumor growth in vivo. Cell Metabolism 17:113—124.
[17] Hirschey, M.D., Berardinis, R.J., Diehl, A.M.E., Drew, J.E., Frezza, C., Green, M.F., et al., Target Validation Team, 2015. Dysregulated metabolism contributes to oncogenesis. Seminars in Cancer Biology 35(Suppl.):S129—S150.
[18] Faubert, B., Vincent, E.E., Poffenberger, M.C., Jones, R.G., 2015. The AMP-activated protein kinase (AMPK) and cancer: many faces of a metabolic regulator. Cancer Letters 356:165—170.
[19] Wheaton, W.W., Weinberg, S.E., Hamanaka, R.B., Soberanes, S., Sullivan, L.B., Anso, E., et al., 2014. Metformin inhibits mitochondrial complex I of cancer cells to reduce tumorigenesis. eLife 3:e02242.
[20] Birsoy, K., Possemato, R., Lorbeer, F.K., Bayraktar, E.C., Thiru, P., Yucel, B., et al., 2014. Metabolic determinants of cancer cell sensitivity to glucose limitation and biguanides. Nature 508:108—112.
[21] Griss, T., Vincent, E.E., Egnatchik, R., Chen, J., Ma, E.H., Faubert, B., et al., 2015. Metformin antagonizes cancer cell proliferation by suppressing mitochondrial-dependent biosynthesis. PLoS Biology 13:1—23.
[22] Scafoglio, C., Hirayama, B.A., Kepe, V., Liu, J., Ghezzi, C., Satyamurthy, N., et al., 2015. Functional expression of sodium-glucose transporters in cancer. PNAS USA 112:E4111—E4119.
[23] Saito, T., Okada, S., Yamada, E., Shimoda, Y., Osaki, A., Tagaya, Y., et al., 2015. Effect of dapagliflozin on colon cancer cell. Endocrine Journal 62:1133—1137.
[24] Matheson, B.K., Adams, J.L., Zou, J., Patel, R., Franklin, R.B., 2007. Effect of metabolic inhibitors on ATP and citrate concent in PC3 prostate cancer cells. Prostate 67:1211—1218.
[25] Ben Sahra, I., Laurent, K., Giuliano, S., Larbret, F., Ponzio, G., Gounon, P., et al., 2010. Targeting cancer cell metabolism: the combination of metformin and 2-deoxyglucose induces p53-dependent apoptosis in prostate cancer cells. Cancer Research 70:2465—2475.
[26] Hawley, S.A., Ford, R.J., Smith, B.K., Gowans, G.J., Mancini, S.J., Pitt, R.D., et al., 2016. The Na+/glucose co-transporter inhibitor canagliflozin activates AMP-activated protein kinase by inhibiting mitochondrial function and increasing cellular AMP levels. Diabetes 65:2784—2794.
[27] Woods, A., Azzout-Marniche, D., Foretz, M., Stein, S.C., Lemarchand, P., Ferre, P., et al., 2000. Characterization of the role of AMP-activated protein kinase in the regulation of glucose-activated gene expression using constitutively active and dominant negative forms of the kinase. Molecular and Cellular Biology 20:6704—6711.
[28] Watt, M.J., Dzamko, N., Thomas, W.G., Rose-John, S., Ernst, M., Carling, D., et al., 2006. CNTF reverses obesity-induced insulin resistance by activating skeletal muscle AMPK. Nature Medicine 12:541—548.
[29] Fullerton, M.D., Galic, S., Marcinko, K., Sikkema, S., Pulinikunnil, T., Chen, Z., et al., 2013. Single phosphorylation sites in Acc1 and Acc2 regulate lipid homeostasis and the insulin-sensitizing effects of metformin. Nature Medicine 19:1649—1654.
[30] The Human Protein Atlas. Stockholm, 2016. http://www.proteinatlas.org [accessed 06.05.15].

[31] Aguer, C., Gambarotta, D., Mailloux, R.J., Moffat, C., Dent, R., McPherson, R., et al., 2011. Galactose enhances oxidative metabolism and reveals mitochondrial dysfunction in human primary muscle cells. PLoS One 6:e28536.

[32] Hawley, S.A., Ross, F.A., Chevtzoff, C., Green, K.A., Evans, A., Fogarty, S., et al., 2010. Use of cells expressing gamma subunit variants to identify diverse mechanisms of AMPK activation. Cell Metabolism 11:554–565.

[33] Dzamko, N., van Denderen, B.J.W., Hevener, A.L., Jorgensen, S.B., Honeyman, J., Galic, S., et al., 2010. AMPK beta-1 deletion reduces appetite, preventing obesity and hepatic insulin resistance. Journal of Biological Chemistry 285:115–122.

[34] Seo, B.B., Kitajima-Ihara, T., Chan, E.K.L., Scheffler, I.E., Matsuno-Yagi, A., Yagi, T., 1998. Molecular remedy of complex I defects: rotenone-insensitive internal NADH-quinone oxidoreductase of Saccharomyces cerevisiae mitochondria restores the NADH oxidase activity of complex I-deficient mammalian cells. PNAS USA 95:9167–9171.

[35] Nomura, S., Sakamaki, S., Hongu, M., Kawanishi, E., Koga, Y., Sakamoto, T., et al., 2010. Discovery of canagliflozin, a novel C-glucoside with thiophene ring, as sodium-dependent glucose cotransporter 2 inhibitor for the treatment of type 2 diabetes mellitus. Journal of Medical Chemistry 53:6355–6360.

[36] Blessing, A., Xu, L., Gao, G., Bollu, L.R., Ren, J., Li, H., et al., 2012. Sodium/glucose co-transporter 1 expression increases in human diseased prostate. Journal of Cancer Science and Therapy 4:306–312.

[37] Effert, P., Berniers, A.J., Tamimi, Y., Handt, S., Jakse, G., 2004. Expression of glucose transporter 1 (Glut-1) in cell lines and clinical specimens from human prostate adenocarcinoma. Anticancer Research 5A:3057–3063.

[38] Menendez, J.A., Lupu, R., 2007. Fatty acid synthase and the lipogenic phenotype in cancer pathogenesis. Nature Reviews Cancer 7:763–777.

[39] Van Baalen, J., Gurin, S., 1953. Cofactor requirements for lipogenesis. Journal of Biological Chemistry 205:303–308.

[40] Schockel, L., Glasauer, A., Basit, F., Bitschar, K., Truong, H., Erdmann, G., et al., 2015. Targeting mitochondrial complex I using BAY 87-2242 reduces melanoma tumor growth. Cancer and Metabolism 3:11.

[41] Pollak, M., 2014. Overcoming Drug development bottlenecks with repurposing: repurposing biguanides to target energy metabolism for cancer treatment. Nature Medicine 5:591–593.

